RESIDUAL STRESS IN THICK GLASS/EPOXY THERMOSET COMPOSITE LAMINATE PLATE MADE BY AUTOCLAVE MANUFACTURING

Mamani, Sara, Hoa, Suong V
Department of Mechanical and Industrial Engineering, Concordia Center for Composites, Montreal, Canada
Center for Research In Polymers and Composites (CREPEC)
* Suong V Hoa (hoasuon@alcor.concordia.ca)
Keywords: *Thick Composite Laminate, Residual Stress, Deep Hole Drilling*

ABSTRACT

Process-induced stress and deformation development in thick thermoset composite laminates can have a major role in decreasing the structural integrity of the components. In the present work, the temperature and cure distributions due to the generated heat during the polymerization of thermoset resin are used to numerically calculate the process-induced thermal gradients in thick 18.28 mm glass/epoxy laminate plates. For this purpose, the finite difference formulation of the one-dimensional transient heat transfer problems was developed. The boundary conditions of the laminate part were simulated to consider the asymmetric condition in the vacuum bag process. The calculated temperature profiles were compared with the experimental result. It was found that the measured temperatures through the thickness agreed well with the numerical values. The overshoot in internal layers led to the temperature and cure gradient which were considered for the residual stress distribution of the thick part.

1 INTRODUCTION

Thick composite laminate structures have been extensively used in various industries such as aerospace and marine. Successful production of respectable quality parts at low cost is key to potential increase of the usage of thick composites. Regrettably, processing history causes unfavorable impacts involving large out-of-plane temperature gradients and mid-plane heat generation. Hence, the residual stress generation due to these gradients during the manufacturing inside the autoclave, can have a major impact on the mechanics and performance of composite structures [1], [2]. Also, issues related to the processing of the thermosetting composites with large thickness associated with the increase of the internal temperatures due to the irreversible exothermic chemical reactions of the matrix phase have been observed. Risk of material degradation is present since there is a slow dissipation of released heat by conduction which can result in internal temperature increase of the part. Another emerging issue is associated with the intricate temperature profiles and varying levels of cure gradients that appear in thick sections during the hardening process [3], [4]. Inadequate solidification in the part can be caused by the non-uniform curing process which can also result in unwanted volume fraction gradients and captured volatiles or voids in the lattice structure [5].This article addresses the one-dimensional finite difference heat transfer formulation of thick thermosetting composites coupled to the cure kinetics of the thermoset composite materials. Then, the process-induced stresses are calculated using the incremental classical laminate theory (ICLT). Moreover, the temperature and process-induced stresses for thick glass/epoxy laminates are calculated and compared with experimental results. It is found that the numerical results have an acceptable agreement with experimental ones.

2 CURE SIMULATION AND HEAT TRANSFER ANALYSIS

2.1 Incremental One Dimensional Finite Difference Heat Transfer Model

To numerically model the experimental set-up and obtain transient temperature profiles and degree of cure distributions across the thickness of glass/epoxy laminates composite, asymmetric boundary conditions are used as illustrated in Figure 1. Also, an incremental transient finite difference method is used. The principal governing differential equation used to analyze the one-dimension heat transfer through the thickness, is expressed as Equation (1):

$$\rho_c C_{c,p}\frac{\partial T}{\partial t}=\frac{\partial}{\partial z}\left(k_{c,t}\frac{\partial T}{\partial z}\right)+q^{\cdot} \tag{1}$$

Here, the parameters T, $k_{c,t}$, ρ_c and $C_{c,p}$ are temperature of any point of the sample at any time, through the thickness thermal conductivity, density and specific heat of the composite, respectively. In this study, these parameters are assumed to be constant during the curing simulation. The term $q^{\cdot}$ is related to the internal heat generation, representing the transient heat liberated per unit volume of material from exothermic chemical reaction due to the cross-link polymerization, expressed according to Equation (2).

$$q^{\cdot}=\rho_c H_u\frac{d\alpha}{dt} \tag{2}$$

Where H_u and $\frac{d\alpha}{dt}$ are the total liberated heat for the complete cure and the rate of cure, respectively. The rate of reaction, $\frac{d\alpha}{dt}$, is a function of degree of cure and temperature. It is required to compute the generated heat and degree of cure during the curing process. A summary of computed thermal properties of glass/epoxy composite are presented in Table 1. The kinetic model utilized in this work is expressed by Equations (3) [6],

$$\frac{d\alpha}{dt}=g(\alpha,T)=(K_1+K_2\alpha^m)(1-\alpha)^n \tag{3}$$

Here, m and n are the reaction orders. The kinetic parameters for glass/epoxy including the pre-exponential coefficients, A_1 and A_2, the activation energies, E_1 and E_2 , universal gas constant, R, are shown in Table 2.

Table 1. Thermal-physical properties of E773/S2glass [7]

	S2-glass	Epoxy	Glass/Epoxy	
Volume fraction (%)	53	47	-	
Thermal conductivity *k* (W/m.K)	0.21	1.04	0.385	
Specific Heat C_p (J/kg.K)	737	1,238	871.545	
Thermal expansion coefficient (10^{-6}/°C)	16	60	$\alpha_1=17.5$	$\alpha_2=59.98$

Table 2. Cure kinetic parameters for glass/epoxy [7]

Parameter	Dimension	Value
A_1	sec^{-1}	55599
A_2	sec^{-1}	72908
E_1	J/mol	58383
E_2	J/mol	51341
m	-	0.58
n	-	1.43

In typical lay-up of autoclaved-cured composites, the stacked prepreg is placed on the tool plate covered by the release film, caul plate, bleeder and the assembly is bagged with a standard nylon bagging as the scheme of boundary condition is shown in Figure 1.

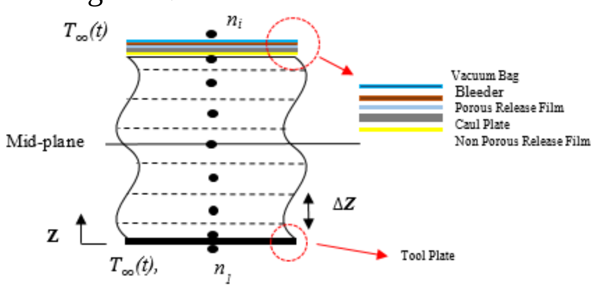

Figure 1 Schematic diagram of the asymmetric boundary conditions.

The effective thermal conductivity of the release film, bleeder and vacuum bag are calculated from the thermal conductivity and thickness of individual components as shown in Equation (4) [8] .

$$k_z^{eff} = \frac{h_{bg} + h_{fl} + h_{bd}}{\frac{h_{bd}}{k_{bd,z}} + \frac{h_{bg}}{k_{bg,z}} + \frac{h_{fl}}{k_{fl,z}}} \quad (4)$$

h_{bg} ,h_{bd} ,h_{fl} ,$k_{bg,z}$, $k_{bd,z}$ and $k_{fl,z}$ are the thickness and thermal conductivity of the vacuum bag, bleeder and release film through the thickness, respectively. The equivalent density for the vacuum bag, bleeder and release film through the thickness is calculated according to Equation (5).

$$\rho_{eq} = \frac{\sum m_i}{\sum V_i} = \frac{A \sum(\rho_i h_i)}{A \sum h_i} = \frac{\rho_{bg} h_{bg} + \rho_{fl} h_{fl} + \rho_{bd} h_{bd}}{h_{bg} + h_{fl} + h_{bd}} \quad (5)$$

Here, ρ_i and h_i are the density and thickness of each material. Table 3 shows the individual material properties used in the asymmetric boundary condition bagging assembly.

Table 3.Thermal-physical properties of the bagging process material [9]

Material	Thermal Conductivity (W/m K)	Specific Heat (J/g K)	Density (g/cm^3)	Thickness(mm)
Aluminum (tp)	220	0.903	2.72	20
Release film (fl)	0.5	1.04	2.2	1
Bleeder (bd)	0.07	1.35	0.26	3
Bag (bg)	0.24	1.67	1.14	1
Aluminum (cl)	220	0.903	2.72	6

The heat balance formulations for each node from the bleeder surface to the bottom layer inside the composite (Figure 1) are expressed according to Equations (6) to (8).

$$k_{cl}A\frac{\partial T_{j-1}^{i}-\partial T_{j}^{i}}{\partial h_{cl}}+k_{z}^{eff}A\frac{\partial T_{j+1}^{i}-\partial T_{j}^{i}}{\partial h_{t}}=(\rho_{eq}C_{Av,p}(\frac{h_t}{2}A)+\rho_{cl}C_{cl,p}(\frac{h_{cl}}{2}A))\frac{\partial T_{j}^{i+1}-\partial T_{j}^{i}}{\partial t} \quad (6)$$

$$k_{fl}A\frac{\partial T_{j-1}^{i}-\partial T_{j}^{i}}{\partial h_{fl}}+k_{cl}A\frac{\partial T_{j+1}^{i}-\partial T_{j}^{i}}{\partial h_{cl}}=(\rho_{cl}C_{cl,p}(\frac{h_{cl}}{2}A)+\rho_{fl}C_{fl,p}(\frac{h_{fl}}{2}A))\frac{\partial T_{j}^{i+1}-\partial T_{j}^{i}}{\partial t} \quad (7)$$

$$k_{c,t}A\frac{\partial T_{j-1}^{i}-\partial T_{j}^{i}}{\partial z}+k_{fl}A\frac{\partial T_{j+1}^{i}-\partial T_{j}^{i}}{\partial h_{fl}}+\rho_{c}H_{u}(\frac{\Delta z}{2}A)\left(\frac{d\alpha}{dt}\right)_{j}^{i}=(\rho_{fl}C_{fl,p}(\frac{h_{fl}}{2}A)+\rho_{c}C_{c,p}(\frac{\Delta z}{2}A))\frac{\partial T_{j}^{i+1}-\partial T_{j}^{i}}{\partial t} \quad (8)$$

2.2 Correlation of Cure Simulation and Experimental Results

The glass/epoxy prepreg used in this work was E773/S-2 Glass. The laminated plate was built up of 80 stacked plies with $152(mm)\times\ 152(mm)\times 18.28\ (mm)$dimensions and cured inside the autoclave using manufactured recommended temperature cure cycle. The temperature variations were measured across the thickness of 80-layer glass/epoxy laminate through embedded thermocouples as shown in Figure 2. A comparison of the temperature profiles obtained from the simulation and experiment are illustrated in Figure 3. It is clear from plots that there is an acceptable agreement between the experimental results and cure simulation predictions. However, a slight difference should be mentioned between the simulation and experimentation results at the second ramp where the overshoot temperature occurs. This could be attributed to the simplified assumptions including but not limited to: the considered and actual kinetic parameters, thermophysical properties of vacuum assembly and its each components thickness. It can also be related to the selected convective heat transfer coefficient between the vacuum bag and autoclave air, disregarded heat transfer enhancement due to the pressure variation during the curing process, etc. It is seen that there is a lag between the overshoots in the second ramp. It takes a little longer that the resulting temperature from simulation to reach its highest value (overshoot temperature). Apparently, the delay is about 13 minutes and the maximum difference between the measured and predicted temperature at its largest value is fairly 10°F which is not considerable and is only 3% of the maximum temperature during the cure cycle. As discussed, this could be due to the difference between the real and considered values for vacuum bag and the thickness of its different components, leading to the difference in the amount of the transferred heat from the boundaries to the laminate plate. Thus, during the process the transferred heat from simulation is slightly larger than that obtained from the thermocouple measurements. Also, it is obvious that there is a delay where the overshoot temperature occurs. This discrepancy could be because that the difference between kinetic parameters. However, the maximum lag along the thickness is less than 5 % of the total cure cycle operating time.

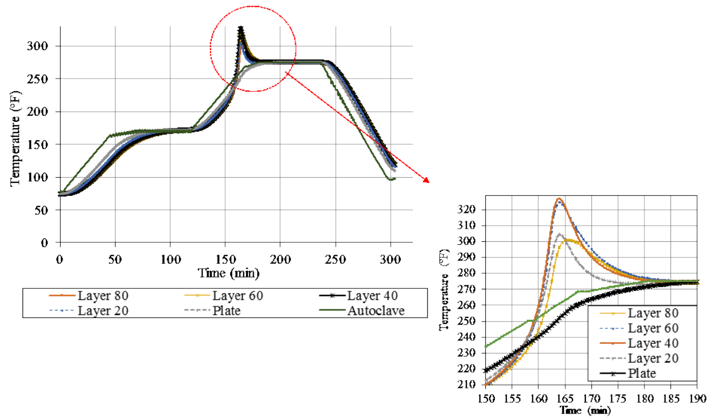

Figure 2 Temperature profile in glass/epoxy laminate from experiment

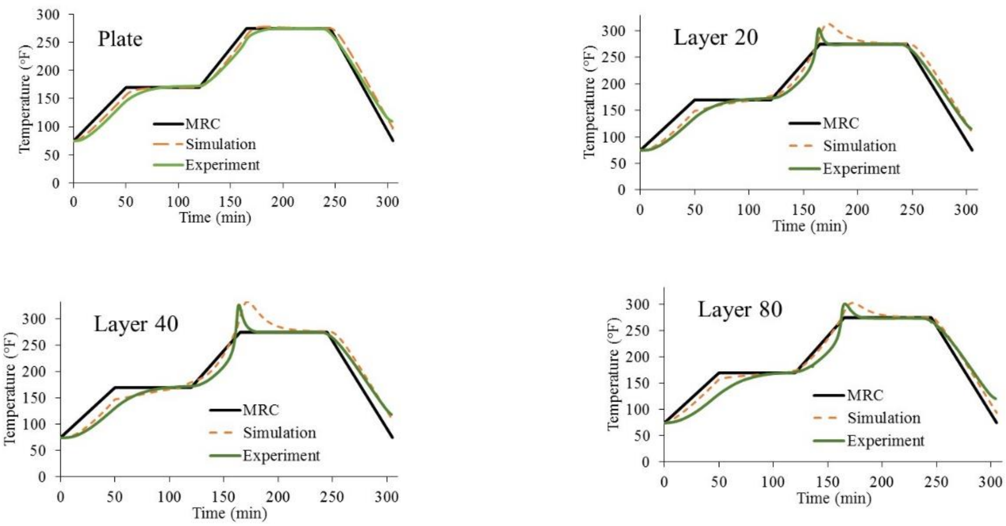

Figure 3 Temperature profiles from experiment and calculated results at different plies.

2.3 Numerical Thermal and Cure Profiles

According to previous studies done by Bogetti [10], it was shown that the laminate thickness and resin system strongly influence the resulting through the thickness temperature and cure gradients. According to their experimental and numerical investigation, it was seen that with an increase in the laminate thickness, a more complex temperature and cure profiles were obtained in the middle layer of the composite part using the symmetric boundary conditions. The temperature profile within glass/polyester laminate also indicates that as the temperature rises, there is a lag and it takes more time as the laminate above 2.54 cm is heating up. However, the resulting temperature profiles in graphite /epoxy laminate parts was shown that by increasing the autoclave temperature and when all the laminates are at exotherm, the mid-thickness temperature rises by an increase in the laminate thickness. Thus, the temperature profile could be varied with different resin system at large thickness due to the conductivity of the composite material which is a function of the composite constituents [9].

In this section, we consider the effect of asymmetric boundary condition and the laminate thickness on the temperature and cure gradients using glass/epoxy laminate plate. An increase in the thickness causes more time for the generated heat to transfer to the central layers during the heat up of the cure cycle compared to the thinner laminates. Since the thermal conductivity of the laminate is small, the dissipation of the liberated heat from exothermal reaction is not carried out easily. Hence, the overshoot temperature and internal temperatures are influenced significantly as the total thickness of the laminate increases.

Figure 4 shows the mid-layer temperature and degree of cure profiles in glass/epoxy laminates for thicknesses between 13.72 mm and 22.86 mm respectively. From temperature profiles, it is apparent that the center of the 13.72 mm laminate follows the autoclave cycle more closely than that of 22.86 mm laminate at the early stages of the cure cycle. Additionally, in order to quantify differences in the curing process of laminates with different thickness, temperature and degree of cure distributions at 164 minutes is demonstrated in Figure 5. As it was calculated, the thicker laminate with the thickness of 22.86 mm has more severe gradients in terms of temperature and degree of cure. It is also clear that the magnitude of the centerline temperature increases with an increase in total laminate thickness and due to the asymmetric boundary condition, the gradients are not symmetric along the centerline of the plate. Hence, the overshoot temperature and internal temperatures are influenced significantly as the total thickness of the laminate increases.

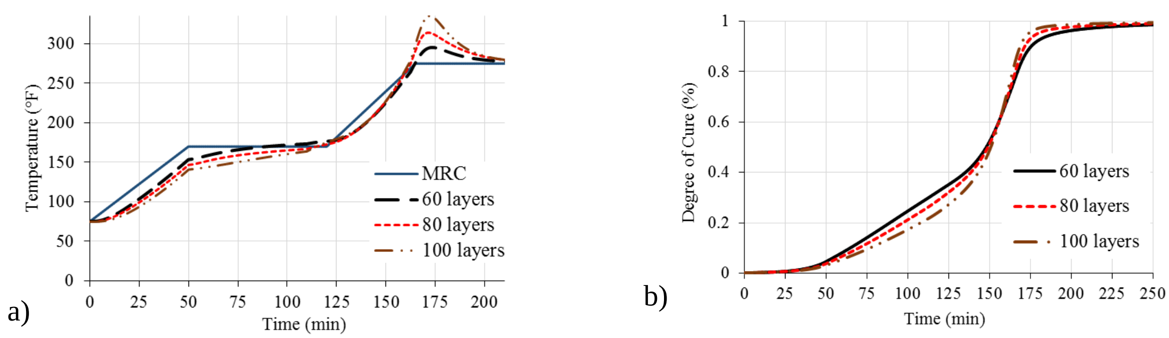

Figure 4 The comparison of the centerline a) temperature b) cure profiles from simulation.

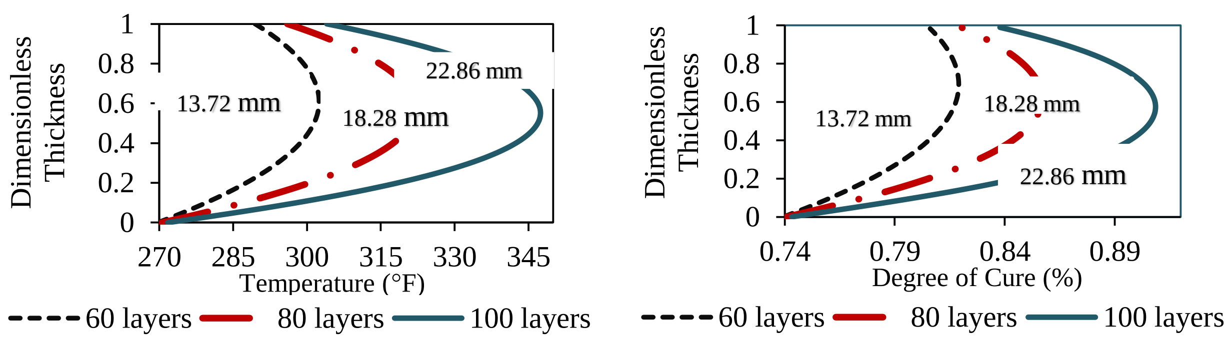

Figure 5 Temperature and cure gradients after 164 min from simulation.

3 RESIDUAL STRESS ANALYSIS IN THICK THERMOSET LAMINATE PLATE

As seen in the previous section, the verification of calculated temperature profile through the thickness in glass/epoxy laminate was conducted. Also, as it was expected, temperature gradients were observed during the curing and cool-down procedure. In this section, the mechanism and procedure developed in an earlier study done by Bogetti [10] is used. The Bogetti`s study addressed the development of macroscopic process-induced stresses in thick composite plates. We also utilize the proposed elastic material models to predict the mechanical properties evolution along with considering processing thermal and chemical strains. Hence, the incremental finite difference model (FD model) is coupled to an incremental classical laminated plate theory (ICLT) [11], to study the evolution of in-plane residual stresses during the cure cycle. Note that in this model, the mechanical and thermal properties of the composite material are calculated at each time increment during the cure cycle. Also, phase transition in thermoset resin system is divided into three different regions during the curing process based on Bogetti's definition: fully uncured (viscous liquid), curing stage, and fully cured (elastic solid). Consequently, this transition in polymer matrix modulus value dramatically influences the mechanical properties of composite laminate during the cure cycle. Note that the development in the resin and lamina modulus is influenced with the degree of cure evolution during the cure cycle and autoclave temperature. That is why for different cure cycles and cured temperature, the modulus growth could be varying in region II.

3.1 Mechanical Properties of glass/epoxy Laminate

An instantaneous cure dependent model to show the evolution of resin modulus was used in Bogetti's study is shown in Equation (9). In this model, the instantaneous isotropic resin modulus, E_m , is expressed in term of degree of cure in region II following as [10]:

$$E_m = (1-\alpha)E_m^0 + \alpha E_m^\infty \tag{9}$$

Here, parameters E_m^0 and E_m^∞ are respectively attributed to fully uncured and fully cured resin modulus. The fully cured and uncured resin moduli are listed in Table 4. In this work, the proposed constitutive model for resin is used to illustrate resin modulus development as demonstrated in Figure 6. Additionally, the evolution of ply mechanical properties illustrated in Figure 7. The obtained mechanical properties from experiment also listed in Table 5. It is also clear from the plot that the magnitude of fully cured modulus is calculated close to the values listed in Table 4 once the fully cure state occurs after 165 min and remained constant afterward.

Table 4. Resin Cure Dependent Characteristic.

Material	E_m^0 **(GPa)**	E_m^∞ **(GPa)** [12]	v_{sh}^T **(%)** [10]
epoxy	3.5e-3	3.5	1-3

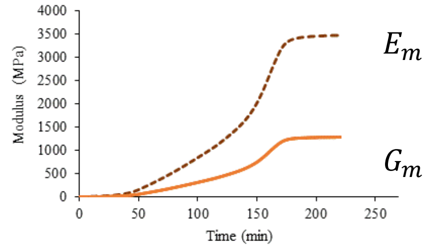

Figure 6 Calculated cure dependent epoxy resin modulus during the curing process

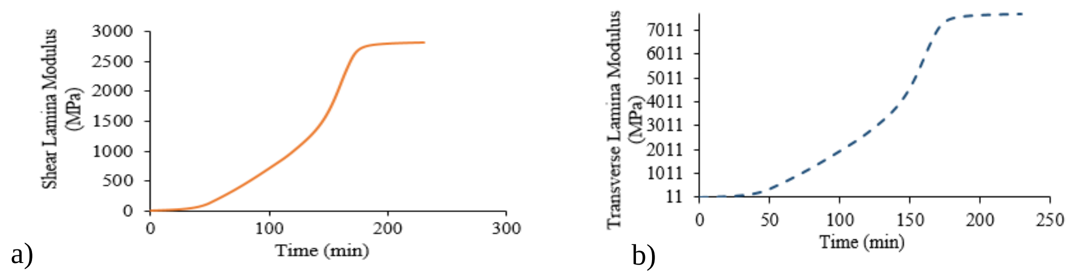

Figure 7 Calculated E773/S2 glass lamina a) shear and b) transverse modulus development during the cure.

Table 5. Mechanical Properties of FX E773/S-2 Glass[13]

Material	**Value (MPa)**
E_1	47930
E_2	11950
G_{12}	4270

3.2 Processing Influential Parameters on Residual Stress Simulation

It is necessary to find the strains which are induced due to the thermal gradients and chemical reactions during the curing process, as the process-induced stresses are governed effectively by the processing stress free strains. Equation (10) shows the isotropic shrinkage strain increment of a unit volume element of polymer matrix, $\Delta\varepsilon^m$ resulted from an incremental volume resin shrinkage, Δv_m expressed in Equation (11). Moreover, the composite shrinkage strain for the lamina is computed incrementally in longitudinal and transverse direction as Equation (12) denoted respectively as $\Delta\varepsilon_1^{ch}$ and $\Delta\varepsilon_2^{ch}$. Also, the instantaneous longitudinal and transvers thermal coefficients of the lamina are obtained based on the micromechanics model as Equation (13) [10]. The transverse shrinkage expansion strains are a function of the resin chemical strain, mechanical properties and the volume fraction of the composite components. The transverse shrinkage and thermal expansion strains of glass/epoxy laminate are shown in Figure 8.

$$\Delta\varepsilon^m = \frac{\sqrt[2]{(1 + 4/3\Delta v_m)} - 1}{2} \tag{10}$$

$$\Delta v_m = \Delta\alpha \times v_{sh}^T \tag{11}$$

$$\Delta\varepsilon_1^{ch} = \frac{\Delta\varepsilon_1^f E_f v_f + \Delta\varepsilon^m E_m(1-v_f)}{E_f v_f + E_m(1-v_f)}$$

$$\Delta\varepsilon_2^{ch} = (\Delta\varepsilon_2^f + \Delta\varepsilon_1^f \vartheta_{12f})\, v_f + (\Delta\varepsilon^m + \Delta\varepsilon^m \vartheta_{12m})(1-v_f) - (\vartheta_{12f} v_f + \vartheta_{12m}(1-v_f))\, \frac{\Delta\varepsilon_1^f E_f v_f + \Delta\varepsilon^m E_m(1-v_f)}{E_f v_f + E_m(1-v_f)} \quad (12)$$

$$\alpha_1 = \frac{\alpha_1^f E_{1f} v_f + \alpha_1^m E_m(1-v_f)}{E_f v_f + E_m(1-v_f)}$$

$$\alpha_2 = (\alpha_2^f + \alpha_1^f \vartheta_{12f})\, v_f + (\alpha_2^m + \alpha_1^m \vartheta_{12m})(1-v_f) - (\vartheta_{12f} v_f + \vartheta_{12m}(1-v_f))\, \frac{\alpha_1^f E_f v_f + \alpha_1^m E_m(1-v_f)}{E_f v_f + E_m(1-v_f)} \quad (13)$$

Then, the incremental principal expansion strains in each ply can be calculated using thermal expansion coefficients and temperature increments between time steps following as:

$$\Delta\varepsilon_1^{th} = \alpha_1 \Delta T$$
$$\Delta\varepsilon_2^{th} = \alpha_2 \Delta T \quad (14)$$

In the above micromechanics model, the fiber and resin Young modulus, chemical shrinkage, Poisson ratio and volume fraction are expressed respectively as E_m, E_f, $\Delta\varepsilon^m$, $\Delta\varepsilon^f$, ϑ_{12f} , ϑ_{12m} and v_f. Table 6 shows fiber and resin constituent mechanical and thermal properties.

Table 6. Mechanical Properties of fiber and resin[10]

Material	Value
E_m (MPa)	Equation 9
E_f (MPa)	7.308e4
v_{12f}	0.22
v_{12m}	0.34

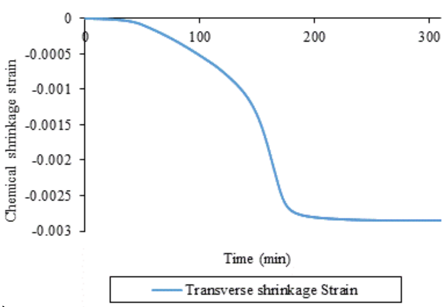

a)

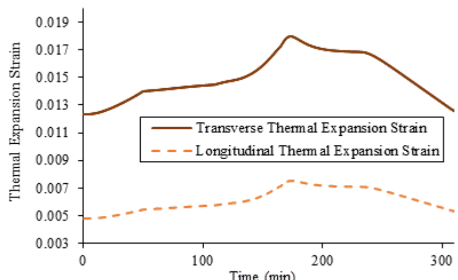

b)

Figure 8 Calculated process stress-free a) transverse shrinkage b) thermal strains in glass/epoxy laminate

3.3 Incremental Laminated Plate Theory

To investigate the influence of the induced temperature gradients on the development of the process-induced stresses, an incremental classical laminated plate theory is used. The stress history is taken into account by accumulated transient process-induced stress and strain along the laminate thickness during the cure simulation and following cool-down to the ambient temperature. In this technique, the laminate is discretized into a distinct number of plies. To uniformly discretize the laminate plate with a distance of z, the midpoint of each two adjacent plies is considered as a node in the finite difference method. As discussed later, a cure simulation was conducted to give the degree of cure and temperature distributions, prior to the plate theory calculations at each time increment. It is notable that the temperature and degree of cure of each ply is calculated using the average of the top and bottom nodes of that ply. According to the resulting temperature and degree of cure distributions, the incremental mechanical properties and macroscopic process-induced strains in each ply are calculated, employing the presented microscopic constitutive models. For each time step of cure simulation, the whole procedure is repeated.

Superposition of the thermal and chemical strain increments gives the total stress-free macroscopic processing-induced ply strain increment as Equation (15). Then, incremental ply process-induced stresses are based on the difference between the ply response strain increments (obtained through laminate response) and the total stress-free process-induced (Equation (15)) strain increments to Equation (16) [10]:

$$\begin{aligned}\Delta\varepsilon_x^{total} &= \Delta\varepsilon_x^{thermal} + \Delta\varepsilon_x^{chemichal} \\ \Delta\varepsilon_y^{total} &= \Delta\varepsilon_y^{thermal} + \Delta\varepsilon_y^{chemical}\end{aligned} \tag{15}$$

$$\begin{aligned}\Delta\sigma_x &= \overline{Q_{11}}(\Delta\varepsilon_x - \Delta\varepsilon_x^{total}) + \overline{Q_{12}}(\Delta\varepsilon_y - \Delta\varepsilon_y^{total}) + \overline{Q_{16}}(\Delta\varepsilon_{xy} - \Delta\varepsilon_{xy}^{total}) \\ \Delta\sigma_y &= \overline{Q_{12}}(\Delta\varepsilon_x - \Delta\varepsilon_x^{total}) + \overline{Q_{22}}(\Delta\varepsilon_y - \Delta\varepsilon_y^{total}) + \overline{Q_{26}}(\Delta\varepsilon_{xy} - \Delta\varepsilon_{xy}^{total}) \\ \Delta\sigma_{xy} &= \overline{Q_{16}}(\Delta\varepsilon_x - \Delta\varepsilon_x^{total}) + \overline{Q_{26}}(\Delta\varepsilon_y - \Delta\varepsilon_y^{total}) + \overline{Q_{66}}(\Delta\varepsilon_{xy} - \Delta\varepsilon_{xy}^{total})\end{aligned} \tag{16}$$

The process-induced transverse stresses for the unidirectional laminate of thickness of 13.71, 18.28 and 22.86 mm were calculated with the total volumetric resin shrinkage, v_{sh}^T, 3% shown in in Figure 9. As can be seen, the parabolic stress profiles show compressive stresses at the exterior and tensile stresses at the interior regions varying between -1.5 MPa and 1.5 MPa. The magnitude and the sign of chemical shrinkage and thermal expansion strains are considered as two important driving forces for the stress development along the thickness. Unlike the composite plates consisting of the polyester resin system [10], it was seen from Figure 8 that in the glass/epoxy laminate case, the shrinkage resin strains are smaller than thermal strains. This leads to the less contribution of the chemical strains in process-induced stresses during the cure cycle. As it was seen from Bogetti's study, the ratio of contribution of the chemical shrinkage strains to thermal strains changes as the total volume resin shrinkage varies from 6% to 0%.

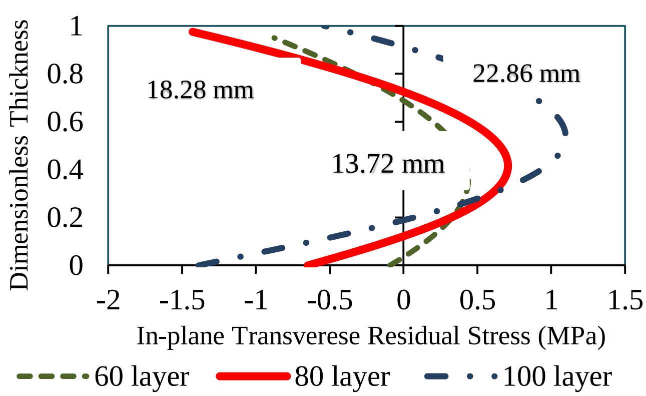

Figure 9 Asymmetric residual process-induced in-plane transverse stress distribution.

The deep hole drilling method was employed to quantify the residual stress in about 18mm unidirectional, $[0]_{80}$, glass/epoxy laminates as numerically studied in the previous section. This experimentation procedure, first, was developed for measurement of residual stresses in isotropic material, then, extended as a practical technique used to study the process-induced stresses in thick composite plate. It consists of the combination of analytical and experimental approach. In this study, the transverse inplane residual stress component was revealed from the radial distortions of the reference hole and compared to that calculated using ICLT model shown in Figure 10.

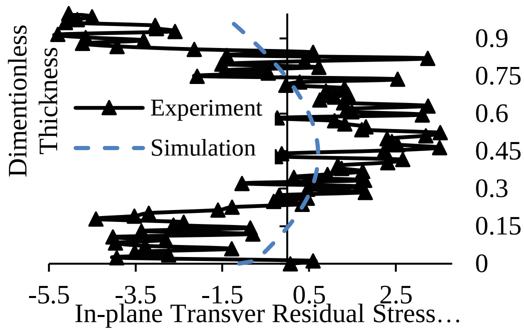

Figure 10 Comparison of in-plane transverse residual stress in unidirectional laminate plate, $[0]_{80}$ [14].

4 CONCLUSION

The investigation on glass/epoxy thick-section laminate composites demonstrates that there is a complex temperature and degree of cure gradients history. It was shown that these gradients can have a significant contribution made towards the process-induced stresses during the manufacturing process inside the autoclave. The evolution of macroscopic in-plane process-induced stresses were studied using incremental cure simulation coupled with classical laminate theory enabling the model to include the temperature gradients during the curing process. Hence, the relationships among temperature and degree of cure gradients and process-induced stress was studied for the thick glass/epoxy composite plates using the asymmetric boundary condition. Also, the deep-hole drilling technique, which previously has developed for the measurement of residual stress in isotropic materials, was used to enable the measurement of residual stress in thick composite laminate plate. It was shown that the predicted stress component exhibited a discrepancy with the experimental results. However, the general trend of the evolution of stresses in the numerical work has an acceptable agreement with the experimental data.

5 REFERENCES

[1] Stango, R. J. and Wang, S. S. "Process-induced Residual Thermal Stresses in Advanced Fiber-reinforced Composite Laminates," *J. Eng for Industry*, 106: 48–54, 1984.

[2] Kau, H. and Petrusha, L. A. "Dimensional Stability and Property Gradients in Thick SMC Sections", *Technical Report GMR-6359, General Motors Research Laboratories*, Warren, MI, 1988.

[3] Levitsky, M. and Shaffer, B. W. "The Approximation of Temperature Distribution in Homogeneous Exothermic Reactions," The Chemical Eng. J., 5: 235–242, 1973.

[4] McGee, S. H. "Curing of Particular Filled Composites," *Polymer Engineering and Science*, 22: 484–491, 1982.

[5] Naji, M. I. and Hoa, S. Y. "Curing of Thick Angle-bend Thermoset Composite Part: Curing Process Modification for

Uniform Thickness and Uniform Fiber Volume Fracture Distribution" *J. Composite Materials*, 34(20): 1710–1755, 2000.

[6] V. Bheemreddy, Z. Huo, and K. Chandrashekhara, "Simulation and validation of cure kinetics for cavity molded composites". *Bell Helicopter Textron, Inc., Fort Worth,* TX 76101, 2013.

[7] V. Bheemreddy, Z. Huo, K. Chandrashekhara, R. A. Brack, B. H. Textron, and F. Worth, "Process optimization of composite flex beams using neural networks," *SAMPE Conference* , Long Beach , CA , May 6-9 , 2013.

[8] JE. OH, "Cure cycle for thick Glass/Epoxy composite laminates," *Journal of Composite Materials,* vol. 36, no. 01, 2002.

[9] Z. GUO, S. DU, and B. ZHANG, "Temperature field of thick thermoset composite laminates during cure process," *Compos. Sci. Technol.*, vol. 65, no. 3–4, pp. 517–523, 2005.

[10] A. Bogetti, and Gillespie J.W.,"Process induced stress and deformation in thick section thermoset composite laminates," *Journal of Composite Materials*, vol. 26, no. 5, pp. 626–660, 1992.

[11] A. A. Johnston, "An integrated model of the development of process-induced deformation in autoclave processing of composite structures," PhD Thesis, University of British Columbia, April 1997.

[12] Cytec engineering material, "Cycom E773 Epoxy Prepreg", Technical data sheet.

[13] Hamid Hamidi, "Static Material Characterization Results S2-E773/ Glass Prepreg", Project report, Mechanical Engineering, Concordia University, 2015.

[14] Sara, M. and Hoa, S. Y. "Measurement of Residual Stress in Thick Thermoset Composite Plates Using Deep Hole Drilling Technique" *21th International Conference on Composite Materials*, 2017.